NASA Technical Memorandum 100072

Laser Doppler Anemometry

Dennis A. Johnson

(NASA-TM-100072) LASER DOPPLER ANEMOMETRY N88-23187
(NASA) 13 p CSCL 20D

Unclas
G3/34 0146030

June 1988

National Aeronautics and
Space Administration

NASA Technical Memorandum 100072

Laser Doppler Anemometry

Dennis A. Johnson, Ames Research Center, Moffett Field, California

June 1988

NASA
National Aeronautics and
Space Administration

Ames Research Center
Moffett Field, California 94035

LASER DOPPLER ANEMOMETRY

by

Dennis A. Johnson

NASA Ames Research Center
Moffett Field, CA 94035, U.S.A

1. INTRODUCTION

Laser Doppler anemometry (LDA) in compressible flows offers the advantages of unambiguous signal interpretation (the laser Doppler anemometer senses velocity only) and nonintrusiveness. Another strength of the LDA is its ability to accurately measure the normal or vertical velocity fluctuations in regions close to a solid surface. This measurement even for zero-pressure-gradient boundary layers is extremely difficult for hot-wire anemometry. Also, LDA is not limited to attached flows with moderate turbulence levels as is hot-wire anemometry.

The primary disadvantage of the technique is that the velocities of micron-size particles are measured rather than the velocity of the fluid itself. In most applications, this requires the introduction of seed particles into the flow (see also Chapter 7). Measurement errors can arise if the particles are not sufficiently small to follow the fluid motions or if they are not uniformly distributed in the flow. Errors also can occur if the signal quality of the photodetector output, which depends on the intensities of the particle-scattered light, is not sufficiently high. Measurements are made difficult because of the rapid fall off in scattered-light intensities with particle diameter. In the particle size range of interest, the intensities decrease nearly with the sixth power of the diameter. Given the current state of the art in lasers and signal processing electronics, the minimum size particles from which measurements can be made at compressible speeds are marginally adequate from a standpoint of trackability.

Another disadvantage of LDA is that it is not well suited for spectra or correlation measurements because of the discontinuous nature of the signal output which is governed by Poisson statistics.

Most LDA compressible boundary-layer measurements have relied on the "dual-beam" (or "fringe") optical arrangement with forward-scatter light collection and burst-counter signal processing. In transonic and supersonic wind tunnels, it is extremely difficult to achieve high particle concentration levels. The dual-beam, burst-counter approach is well suited to applications such as these where the particles are sparsely distributed. There are a vast number of papers in the literature describing various aspects of LDA, numerous technical meetings have been dedicated just to LDA and several books have been written on the subject. The intent of this chapter is to discuss some of the more relevant aspects of applying LDA (specifically, the dual-beam, burst-counter approach) to compressible flows.

2. BASIS OF DUAL-BEAM, BURST-COUNTER LDA SYSTEMS

A simplified dual-beam arrangement for single-component velocity measurements is shown in Fig. 1. In this configuration, the collecting lens is positioned to collect only particle-scattered light from the two incident laser beams. In earlier LDA systems, the Doppler signal was obtained by heterodyning non-scattered light from one of the incident beams with particle-scattered light from the other beam. This approach had the disadvantages of being sensitive to mechanical vibrations and of requiring small light-collection solid angles. The dual-beam arrangement does not have these disadvantages. Early analyses of the dual-beam optical arrangement were performed by Rudd (1969), and Mazumder and Wankum (1970).

With the availability of the argon-ion laser in the early 1970s high-speed LDA measurements became realizable. It provided the additional laser power (more than two orders of magnitude over the standard helium-neon laser) needed to detect individual submicron particles traveling at the speed of sound or higher with the dual-beam optical arrangement. From the oscilloscope traces of signal bursts produced from individual particles, came the idea of using high-speed counters to measure the velocity of individual particles crossing the sensing volume. The earliest work on the burst counter approach was performed by a research group at AEDC, Arnold Air Force Station, Tenn. (Lennert, et al., 1970).

An alternative approach to using burst counters is that of photon correlation (Abbiss, 1976) which is capable of working with much lower scattered light levels. Another, is the digitization of the signal bursts followed by signal analysis via a digital computer (Peterson and Maurer, 1975). By Fourier transforming the digitized signals, measurements by this approach can be obtained from signals too noisy to be processed by a burst counter. However, neither approach has attained the same level of popularity in compressible flow applications as the burst counter. One reason for this has been the lower signal frequency limits of these approaches compared to those for burst counters. Also, both techniques require substantial computer postprocessing.

The dual beam arrangement is often referred to as the fringe arrangement because of the fringe pattern which is formed by the mutual interference of the two (ideally of equal intensity) incident laser beams. This fringe pattern is depicted in Fig. 2. These fringes are parallel to the bisector of the two incident beams and perpendicular to the plane formed by the two incident beams. The spacing of the fringes x_f is given by $x_f = \lambda/2 \sin \theta/2$ where θ is the angle between the two incident beams and λ is the wavelength of the laser light. The electrical signal, e(t) produced at the photodetector by an individual particle crossing these fringes has the form:

$$e(t) = \frac{1}{2} e^{-gt^2} \left(1 + \cos \frac{2\pi u_1}{x_f} t\right) \tag{1}$$

where the envelope function g depends on the trajectory of the particle passing through the sensing volume, u_1 is the velocity component perpendicular to the interference fringes, and t is time in Eq. 1. Passing this signal through a high-pass filter produces a signal given by

$$e(t) = \frac{1}{2} e^{-gt^2} \cos \frac{2\pi u_1}{x_f} t \tag{2}$$

that is symmetric with respect to zero and which crosses zero at fixed time intervals of $\tau_0 = (1/2)\, x_f/u_1$.

In compressible flow applications, θ is made relatively small (1 to 2°) so the signal frequencies do not exceed the capabilities of the photodetector or the signal processing electronics. If the laser is not operated in single mode, then high-frequency noise from the laser also becomes a consideration in limiting the maximum signal frequency (Dopheida and Durst, 1979). Typical fringe spacings are in the 10 to 30 μm range in compressible flow studies.

Because θ and the light collection angle, α (Fig. 1) are both relatively small in compressible flow applications, the sensing volume is highly elongated in the direction of the optical axis (i.e., the bisector of the two incident laser beams). Its shape is ellipsoidal with a Gaussian cross-sectional intensity distribution. The aspect ratio of the ellipsoid can be as large as 50 but likely never less than 10. The effective diameter, which is determined by the diameter of the laser beams ahead of the transmitting lens and the transmitting lens focal length, is typically between 200 and 400 μm. The upper frequency limit of the signal processing electronics restricts how small the sensing volume can be.

Forward-scatter light collection refers to the case where α in Fig. 1 is small while in back-scatter configuration, α, is near 180°. In wind tunnel applications, the forward-scatter configuration generally requires that the light-collection optics be placed on the opposite side of the tunnel test section from that of the transmitting optics. Although this makes for mechanical inconveniences, experience has shown that the gain of about two orders of magnitude in light scattered intensities over that for back scatter is essential in the transonic and supersonic regimes when burst counters are used for signal processing.

The burst counter is designed to filter out the low-frequency component in Eq. 1 and then measure the average period of a given number of cycles of the signal (eight cycles is the most common). Pulses from a high-frequency clock (up to 1 GHz) are counted to determine the average period. The number of cycles used is a compromise between resolution and frequency limitations.

In the study of compressible boundary-layer flows, the two-velocity component systems which use the two strong lines (4880 and 5145 Å) of the argon-ion laser are the most popular. These two laser lines are sufficiently apart that signal separation at the detectors can be accomplished by optical filtering. With this system, four laser beams (two with $\lambda = 4880$ Å and two with $\lambda = 5145$ Å) are brought to a common focus with a single transmitting lens. The results are overlapping sensing volumes whose fringes are orthogonal. Usually a shift in frequency, f_B is introduced into each pair of beams which causes the fringes to move at a constant velocity, $v_f = x_f f_B$. With this fringe motion, forward and reverse velocities can be distinguished.

While frequency shifting is obviously important in the measurement of separated flows, it can be important even in moderately high turbulent flows when burst counters are used. Depending on the turbulence level, the number of fringes in the sensing volume, and the minimum number of fringe crossings required by the burst counter, there is the possibility that certain particles will not cross a sufficient number of fringes to be measured. In which case, measurement errors can occur. The use of frequency shifting, if properly applied, can prevent this possibility. The observed fall-off of the near-wall Reynolds shear stresses in early studies (Johnson and Rose, 1975; Yanta and Lee, 1974; and Dimotakis et al., 1979) of zero-pressure-gradient compressible boundary layers appears to have been at least partly the result of not using frequency shifting (Schairer, 1980; and Robinson et al., 1983).

3. SIGNAL PROCESSING ASPECTS

The major difficulty in the application of LDA is that the signals from the photodetector are relatively noisy even under ideal situations. This is further complicated in high-speed applications because

of the need for smaller light scatterers for particle tracking and the reduced residence time of the particles in the sensing volume. The signal-to-noise ratio (SNR) for an LDA signal, defined as the ratio of signal power to noise power, is approximately given by the following expression:

$$SNR = \frac{\eta}{h\nu} \cdot \frac{P_S}{(1 + P_B/P_S)\Delta f} \tag{3}$$

where η is the quantum efficiency of the photodetector, $h\nu$ is the energy of a single photon, P_S is the particle-scattered light power, P_B is the background light power, and Δf is the instrument bandwidth. This expression assumes there are many photoelectrons-per-filter resolving interval; i.e., the signals are sufficiently strong as not to be photon resolvable.

The particle-scattered light power depends on the incident laser intensity, the Mie scattering function of the particle, and the location and F number of the collection lens. In general, P_S drops dramatically with particle size as will be discussed in the next section. The penalty paid by the burst counter's ability to measure the frequency of individual scatters in a highly turbulent flow is its wide bandwidth (large Δf) which increases the noise in signal. The required instrument bandwidth for turbulent flow measurements depends on the highest expected measurement speed and the fringe spacing. Hence, the need for smaller particles reduces P_S while the greater speeds demands an increase in Δf, both of which result in reduced SNRs. The variable P_B represents the total of all undesired laser light which enters the detector. This generally will be laser light which is scattered from optical components, wind tunnel windows and model surfaces. Well designed LDA systems using low-loss optics attempt to minimize the collection of this stray light but it cannot be completely eliminated. The deterioration in SNR caused by stray light can be acute when measurements are attempted close to model surfaces. In compressible flow applications, an SNR of 100 (20 dB) would be considered quite respectable.

Burst counters have been designed to have some noise rejection capabilities; however, the signals must be relatively clean or erroneous measurements can occur. All of the commercially available burst counters have a threshold level which determines the minimum level signal the counter will attempt to process. The threshold level is normally set well above the switching level of the Schmidt trigger which converts the signal into a series of square waves. Either the threshold level is directly adjustable or indirectly via a variable gain control on the preamplifier. Without this threshold level capability, measurements are virtually impossible.

Other noise rejection techniques commonly used include 1) a comparison of the average period of four or five signal cycles to that for eight cycles (other variations on this four/eight or five/eight comparison are now available), and 2) a three-level comparison which requires that the signal passes a + level, 0 level and - level in the proper sequence. Of these two methods of noise discrimination, it has been the writer's experience that the three-level comparison is more effective in eliminating noisy signals than the four/eight or five/eight cycle comparison. As a rule however, any burst counter will give erroneous output if it is required to process signals which are sufficiently noisy. For example, a burst counter can generate output from just the shot noise of the detector--the laser does not even have to be on to obtain data.

In practice, an attempt is made to set the threshold level sufficiently high so all the signal bursts satisfy the signal quality requirements of the counter, and yet sufficiently low that an acceptable dat rate is achieved. Generally the SNRs of the signal bursts are not measured in an experiment (this can be done by digitizing and then Fourier transforming the signal bursts). Usually, measurements in the free-stream of the flow of interest (where the turbulence levels are known to be low) are made to test whether the signal qualities are sufficiently good for reliable measurements. In practice, the mimimum recordable rms with an LDA is almost without exception governed by signal quality (i.e., SNR) and not the clock rate of the burst counter. Although there are too many variables to extract an exact relationship between SNR and measurement uncertainty, it is reasonable to expect the minimum measurable rms to depend inversely on the square root of the SNR (Mayo, 1979; and Binder et al., 1986). The lowest free-stream root mean square (rms) observed by this writer in compressible experiments has been 1% (the actual turbulence levels were considerably less). These were cases where the frequency bandwidth was large since the flows of interest were highly turbulent.

Care must be taken when measurements closer to a solid surface are attempted since the SNRs will generally be lower because of an increase in P_B. When the background light level increases, a common practice is to raise the threshold level so that only the strongest signals are processed. Often a real-time observation of the output in histogram form is used to help detect bad readings and to set the threshold of the counters.

Because of the noise-in-signal effects, the LDA is not well suited for measuring very low turbulence levels. The measured rms can be reduced to some extent by using two counters to measure the same signal or even better, signals from two different photodetectors and then cross correlating their outputs as suggested by Lau et al. (1981). The accuracy of mean-velocity measurements can be significantly better than the minimum measurable rms if the noise effects produce a Gaussian probability density function (pdf). This theoretically will be the case if the SNRs are reasonably high (Cobb, 1965).

4. PARTICLE LIGHT SCATTERING AND TRACKING

For the realization of accurate LDA measurements, particle lag effects must be negligibly small (see also Chapter 7). To the accuracy of Stokes's drag law, the time constant (i.e., the 1/e point) for a particle subjected to a discontinuous change in gas velocity is given by

$$\tau_c = \frac{\rho_p d_p^2}{18\mu_g} \tag{4}$$

where ρ_p and d_p are the particle density and diameter, respectively and μ_g is the viscosity of the gas. For fixed fluid properties and particle density, the particle response is proportional to the square of the particle diameter. Analogous to the 3-dB frequency response quoted for hot-wire anemometry, but in the moving reference frame of the particle, the particle response is given by $f_{3dB} = 1/2\pi\tau_c$. If we assume the step change in velocity to be small, the response distance x_c can be expressed as $x_c = u_g\tau_c$ where u_g is the speed of the flow.

Values of f_{3dB} and x_c are given in Table 1 for different sizes of particles with a specific gravity of unity in a Mach 3 flow with a 293 K stagnation temperature. For lower Mach numbers, these values improve because of the decrease in u_g and the increase in μ_g (e.g., μ_g is 2.5 times larger at ambient temperature conditions). For low-density flows as encountered in hypersonics, a correction for mean-free path relative to particle diameter must be made (Becker et al., 1967) in which case the time constant is given by

$$\tau_c = \frac{\rho_p d_p^2}{18\mu_g}\left(1 + k\,\frac{L}{d_p}\right)$$

where L is the mean free path and k is the Cunningham correction; $k = 1.8$ for air. When the Knudsen number is large, the particle response goes as the particle diameter rather than the particle diameter squared. Because of this, Owen and Calarese (1987) suggest that an optimum seeding particle in some hypersonic flows may be one that is nominally larger than normally used in LDA, but which has a much lower specific gravity.

Since the particles are convected in the Lagrangian frame, it is difficult to assess how large the particles can be, and still have negligibly small particle lag relative to the turbulent fluctuations. Mean convective speeds of the turbulent eddies in a zero-pressure-gradient turbulent boundary layer are all within 20% of the local mean velocity. This suggests that for a zero-pressure-gradient boundary layer the relevant frequency response could be a factor of five larger than those given in Table 1. Supporting evidence that the frequency responses given in Table 1 are overly conservative comes from the study of Yanta and Lee. In that study, reasonably accurate mean velocities and Reynolds stresses were obtained in a supersonic turbulent boundary layer using 5 μm seed particles. Obviously, the effective response of these 5 μm particles must have been better than the 0.9 kHz quoted in Table 1.

Rapid spatial changes (such as that caused by shocks) or sustained strong streamwise curvature are of more concern than the response to convected turbulence fluctuations. Although locally the particle speeds may be very close to that of the surrounding fluid in the situation of sustained streamwise curvature, substantial particle concentration gradients can result which in turn can produce a biased sample of the flow statistics. (The author is not aware of any studies which have addressed this potential problem.)

To illustrate the advantages of forward scatter over back scatter and the rapid fall off in scattered-light intensities with particle diameter, results (taken from van de Hulst, 1957; and Gumprecht et al., 1952) based on Mie scattering calculations are shown in Fig. 3. Light scattering intensities, i, for water droplets (index of refraction, $n = 1.33$) exposed to 0.5 μm wavelength light for forward scatter ($\alpha = 0°$) and back scatter ($\alpha = 180°$) are plotted as a function of particle diameter. Up to $d = 0.5$ μm it is seen that the forward scatter intensity varies very nearly as the sixth power of the particle diameter as predicted by Rayleigh-scattering theory. This is somewhat surprising since Rayleigh scattering is theoretically only valid for $d \ll \lambda$. A common seed particle in LDA are polystyrene spheres ($n = 1.55$), and these particles show a similar behavior. The water droplet results are shown because more extensive Mie scattering calculations were available. For a given size particle, Fig. 3 shows that the scattering intensities in forward scatter are approximately two orders of magnitude larger than those in back scatter. This is significant since Eq. 3 states that this results in two orders of magnitude difference in SNR (P_S is determined by integrating i over the solid angle of light collection). On the other hand, if the minimum acceptable intensity for accurate velocity meaurements were, for example, $i = 60$ then a 0.5 μm particle could be measured in forward scatter according to Fig. 3, while in back scatter measurements would be limited to 2 μm or larger particles. If the system sensitivity were considerably less, say $i = 600$, then particles as small as 0.8 μm could still be sensed in forward scatter, but in back scatter, the particles would have to be 6 μm or larger (this is based on calculations which are off the scale of Fig. 3). Clearly, substantial gains in sensitivity result from using forward scatter.

Because the intensities fall so rapidly for $d_p < 1$ μm, it is difficult to effect any significant improvements in the mimimum size particle that can be measured. Below $d_p = 0.5$ μm for example, an order

of magnitude increase in incident laser power would only result in a 33% reduction in diameter of the smallest detectable particle.

The problem is compounded by the fact that it is nearly impossible to generate an aerosol which does not contain some particles which are larger than desired. Since these larger particles will scatter more light, they will have a higher probability of being measured than a smaller particle. The recent Mach 3 compression corner study of Kuntz et al. (1987) exemplifies the difficulty of generating sufficiently small particles for trackability yet large enough for detection. Measurements across an oblique shock at Mach 3 showed that the effective diameters of the oil droplets used for light scattering in that study were between 1.5 and 2 μm. These particles have to be considered definitely borderline in the study of supersonic shock-wave/boundary-layer interaction flows. In the Mach 3 shock-induced separation study of Modarress and Johnson (1979), aerodynamic diameters of 0.5 μm were confirmed from shock-wave response measurements. Realistically, this is about as small a particle that can be used in supersonic measurements when burst counters are used to process the signals.

5. DATA REDUCTION AND SAMPLING BIAS

Most commonly, the flow statistics are calculated from the burst counter output based on the assumption that the sampling is random. Thus, the possibility of a sampling bias toward higher velocity particles as first discussed by McLaughlin and Tiederman (1973) is generally ignored. This bias is argued to occur when particle concentrations are low because more fluid is swept through the sensing volume during periods of high velocity than periods of low velocity which thus enhances the possibility of high-velocity samples over that for low-velocity samples. Although this bias has been verified in numerous low-speed studies (Stevenson et al., 1982; Johnson et al., 1984; and Binder et al., 1986) and evidence of its existence in high-speed flows has been presented (Petrie et al., 1985), there has been a reluctance to correct results for this bias. Fortunately, the effect of this sampling bias when present is negligibly small at moderate turbulence levels (say less than 20%). The reluctance to correct for sampling bias stems from the conflicting results that have been reported in the literature. Also, there is the possibility of compensating errors because of inadequate photodetector response (Durao et al., 1980). This effect, though, should be minimal when frequency shifting is used.

One way to avoid the effects of sampling bias is to heavily seed the flow such that particle interarrival times are much less than the turbulence time scale and then restrict the sampling of the counter to much longer, fixed sample times (Stevenson et al., and Edwards and Jensen, 1983). However, this is not practical in high-speed applications. Edwards and Meyers (1984) proposed that the degree of sampling bias be determined by measuring the mean sample rate as a function of the velocity over periods short relative to the turbulence time scales. With this information available corrections to the uncorrected pdf's can be made. This again requires data rates beyond that which can be obtained in compressible flows. Moreover, there is an additional problem with this proposal because of the relatively long sensing volumes of most LDA systems. If the sensing volume is long relative to the turbulence scales, then even if sampling bias was present little correlation between sample rate and velocity would be apparent. Chen and Lightman (1985) using this approach, observed a very strong correlation between velocity and mean sample rate for a low-speed centerbody flow. But in that study, the flow was dominated by very large vortical structures (their scales were large even compared to the 5-mm length of the sensing volume).

Theoretically, if the sensing volume is cylindrical in shape and of a high aspect ratio (this is a good approximation to the actual ellipsoidal sensing volumes), the mean and rms velocities based on N samples should be calculated using the following formulas (for brevity, only the expressions for the streamwise velocity component u are given):

$$\bar{u} = \sum_{i=1}^{N} \omega_i u_i \Big/ \sum_{i=1}^{N} \omega \tag{6}$$

and

$$\langle u' \rangle = \frac{\sum_{i=1}^{N} \omega_i \, (u_i - \bar{u})^2}{\sum_{i=1}^{N} \omega}^{1/2} \tag{7}$$

where ω is a weighting factor given by

$$\omega = \frac{1}{\rho}\left[\left(u_i^2 + v_i^2\right)^{1/2} + \frac{\pi}{4} \cdot \frac{d}{\ell} \cdot w_i\right]$$

In this expression, ρ is the fluid density; and v and w are the normal and cross stream velocity components, respectively; and d and ℓ are the diameter and length of the cylindrical sensing volume. Under the assumption of no sampling bias $\omega = 1$.

Although density fluctuations can theoretically affect the sampling bias as seen from Eq. 8, they are ignored when corrections are made for sampling bias. For high Mach number flows, their effect could become important. Also, since the cross stream velocity component w_i is not usually measured, the last term in Eq. 8 is either ignored or estimated (Nakayama, 1985) in terms of $\langle u' \rangle$ and $\langle v' \rangle$. Because d/ℓ is usually quite small, this term is normally small compared to the other two terms.

The possible measurement errors due to sampling bias increase with turbulence intensity. Shown in Fig. 4 are results for a transonic, shock-wave/turbulent-boundary-layer interaction on an axisymmetric bump obtained using ω_i given by Eq. 8 (with w neglected) and using $\omega_i = 1$. Except in the separated flow region (maximum separation occurred at the bump trailing edge), the differences are probably within the accuracy of the measurements. And even there, the maximum difference in mean velocity is only 5% with respect to the edge velocity. The largest differences were observed in the $\overline{u'v'}$ measurements. Similar trends to those shown in Fig. 4 were observed by Petrie et al. (1985) for a supersonic base flow.

The issue of sampling bias has yet to be resolved within the LDA scientific community. At the present time, the two approaches given previously must be thought of as a bound on the data. This suggests that the data be reduced in both ways to check the possible effects sampling bias could have on the results. Given that both u and v are measured simultaneously, which is the most accurate way of determining the shear stress $\overline{u'v'}$, little additional effort is needed to reduce the data using both formats. At very high Mach numbers, the potential effect of density fluctuations on the sampling bias adds another level of uncertainty.

6. THREE-DIMENSIONAL MEASUREMENTS

The measurement of the third velocity component, w, in a three-dimensional turbulent boundary layer with an LDA is extremely difficult. As discussed earlier, with the "dual beam" optical arrangement the measured velocity component is perpendicular to the bisector of the two incident beams. Since in most wind tunnels, optical access is from the sides of the test section the measurement of u and v are straightforward. Such is not the case for the measurement of w.

In boundary-layer studies, it is best to have the laser beams come in at a grazing incidence to the surface of interest to reduce background scattered light. The most common procedure in three-dimensional applications has been to have a third pair of beams (of either a third color, a different polarizaion or frequency shifted) which lie in the same plane as the pair of beams used to measure u, but which make a substantial angle ψ with respect to these beams (Fig. 5). The velocity component sensed, in this case, is $r = u \cos\psi + w \sin\psi$. In wind tunnel applications, the angle ψ is normally restricted because of limitations in optical access. This limits the resolvability of w. To improve resolution, electronic mixing of the signal dependent only on u with the signal dependent on u and w was performed by Asherman and Yanta (1984). In this procedure, the fringe spacings are adjusted so that the difference frequency of the two signals depends only on w. Besides the added complexity of this approach, it has the disadvantage that the SNR of the mixed signal is considerably reduced from that of the original two signals which causes other measurement uncertainties. It also does not circumvent the basic problem of reduced sensitivity to w caused by ψ being small.

An additional complication in three-dimensional measurements arises because of the small overlap region of the third velocity component beams relative to the original sensing volume for u and v (Fig. 5). Even when coincidence between all three components is required to affect a measurement, there is a relatively high likelihood that the measurement will be from two particles (one or both of which are not in the overlap region) if the overlap region is small relative to the individual sensing volumes. In which case, in addition to the desired velocity component pairs $(u_i, r_j : i = j)$ obtained from the same particle, velocity component pairs $(u_i, r_j : i = j)$ generated by two particles are measured. Boutier et al. (1985) refer to these latter velocity component pairs as "virtual" particles and show that they can produce significant overestimations in $\overline{w'w'}$. Driver and Hebbar (1987) in a low-speed boundary layer study found this virtual particle problem for ψ equal to 60° to result in an underestimation of $\overline{w'v'}$ by 20%. This represents a serious problem which will need to be addressed in future high-speed, three-dimensional boundary-layer studies.

7. CONCLUDING REMARKS

Much has been accomplished with LDA in compressible flows despite the difficulties posed by the high speeds and additionally by the rapid spatial changes in speed or flow direction in some cases. The successful application of the technique is difficult because the SNRs are fairly low even under the best of conditions and highly variable because of variations in particle size and particle location within the sensing volume. And, the available signal processing is not very effective in discarding signals that are too noisy to provide an accurate velocity measurement. The temptation is to work with particles which are too large to adequately follow the flow but which provide cleaner signals due to increased scattering intensities. For the data to have credibility, some check on the particle response must be made for a given facility and LDA system. The capability, if developed, of being able to determine the size of each particle upon which a measurement is based and the SNR of the corresponding signal burst would be extremely valuable in reducing much of the uncertainty now present in LDA compressible flow measurements.

8. REFERENCES

Abbiss, J. B. (1976), Development of photon correlation anemometry for application to supersonic flows. AGARD CP 193.

Ausherman, D. W. and Yanta, W. J. (1984), The three-dimensional turbulent transport properties in the boundary layers of conical body configurations at Mach 3. AIAA P-84-1528.

Becker, H. A., Hottel, H. C., and Williams, G. C. (1967), On the light-scatter technique for the study of turbulence and mixing. J. Fluid Mech. 30, pp. 259-284.

Binder, G., Tardu, S., and Blackwelder, R. (1986), An experimental investigation of LDA biasing using a large amplitude oscillatory channel flow. Third Int. Symp. Applications of Laser Anemometry to Fluid Mech., Lisbon, Portugal.

Boutier, A, Pagon, D., and Soulevant, D. (1985), Measurements accuracy with 3D laser velocimetry. Int. Conf. on Laser Anemometry - Advances and Application, Manchester, England.

Chen, T. H. and Lightman, A. J. (1985), Effects of particle arrival statistics on laser anemometer measurements. Int. Symp. Laser Anemometry, ASME Winter Annual Meeting, Miami Beach, Florida.

Cobb, S. M. (1965), The distribution of intervals between zero-crossings of sine- wave plus random noise and applied topics. IEEE Trans. Info. Theory IT-11, pp. 220-233.

Dimotakis, P. E., Collins, D. J., and Lang, D. B. (1979), Laser Doppler velocity measurements in subsonic, transonic and supersonic turbulent boundary layers. Laser Velocimetry and Particle Sizing, Hemisphere, Washington, D.C.

Dopheide, D. and Durst, F. (1979), High speed velocity measurements using laser Doppler anemometry. Laser Velocimetry and Particle Sizing, Hemisphere, Washington, D.C.

Driver, D. M. and Hebbar, S. K. (1987), Experimental study of a three-dimensional, shear-driven, turbulent boundary layer. AIAA J. 25, pp. 35-42.

Durao, D. F. G., Laker, J., and Whitelaw, J. H. (1980), Bias effects in laser Doppler anemometry. J. of Phys. E: Sci. Instrum. 13, pp. 442-445.

Edwards, R. V. and Jensen, A. S. (1983), Particle-sampling statistics in laser anemometers: sample-and-hold systems and saturable systems. J. Fluid Mech. 133, pp. 397-411.

Edwards, R. V. and Meyers, J. F. (1984), An overview of particle sampling bias. Second Int. Symp. Applic. Laser Anemometry to Fluid Mech., Lisbon, Portugal.

Gumprecht, R. O., Sung, N., Chin, J. H., and Sliepcevich, C.M. (1952), Angular distribution of intensi' of light scattered by large droplets of water. J. Optical Soc. of Amer. 42, pp. 226-231.

Johnson, D. A. and Rose, W. C. (1975), Laser velocimeter and hot-wire anemometer comparison in a supersonic boundary layer. AIAA J. 13, pp. 512-515.

Johnson, D. A., Modarress D., and Owen, F. K. (1984), An experimental verification of laser-velocimeter sampling bias and its correction. J. Fluids Eng. 106, pp. 5-12.

Kuntz, D. W., Amatucci, V. A., and Addy, A. L. (1987), Turbulent boundary-layer properties downstream of the shock-wave/boundary-layer interaction. AIAA J. 25, pp. 668-675.

Lau, J. C., Whiffen, M. C., Fisher, M. J., and Smith, D. M. (1981), A note on turbulence measurements with a laser velocimeter. J. Fluid Mech. 102, pp. 353-366.

Lennert, A. E., Brayton, D. B., Crosswy, F. L., Smith, F. H. Jr., and Kalb, H. T. (1970), Summary report of the development of a laser velocimeter to be used in AEDC wind tunnels. AEDC-TR-70-101.

Mayo, W. T., Jr. (1979), Ocean laser velocimetry systems: signal processing accuracy by simulation. Laser Velocimetry and Particle Sizing, Hemisphere, Washington, D.C.

Mazumder, M. K. and Wankum, D. L. (1970), SNR and spectral broadening in turbulence structure measurement using a CW laser. Appl. Optics 9, pp. 633-637.

McLaughlin, D. K. and Tiederman, W. G. (1973), Biasing correction for individual realization of laser anemometer measurements in turbulent flow. Phys. Fluids 16, pp. 2082-2088.

Modarress, D. amd Johnson, D. A. (1979), Investigation of turbulent boundary-layer separation using laser velocimetry. AIAA J. 17, pp. 747-752.

Nakayama, A. (1985), Measurements of separating boundary layers and wake of an airfoil using laser Doppler velocimeter. AIAA P-85-0181.

Owen, F. K. and Calarese, W. (1987), Turbulence measurements in hypersonic flow. AGARD CP 428.

Peterson, J. C. and Maurer, F. (1975), A method for the analysis of laser-Doppler signals using a computer in connection with a fast A/D-converter. Proceedings of the LDA Symposium Copenhagen 1975, Hemisphere, Washingon, D.C.

Petrie, H. L. Saminy, M. and Addy, A. L. (1985), An evaluation of LDV velocity and fringe bias effects in separated high speed turbulent flows. International Congress on Instrumentation in Aerospace Simulation Facilities, Stanford, CA, IEEE Publication 85CH2210-3.

Robinson, S. K., Seegmiller, H. L., and Kussoy, M. I. (1983), Hot-wire and laser Doppler anemometer measurements in a supersonic boundary layer. AIAA P-83-1723.

Rudd, M. J. (1969), A new theoretical model for the laser Dopplermeter. J. Phys. E. Sci. Instrum. 2, pp. 55-58.

Scharier, E. T. (1980), Turbulence measurements in the boundary layer of a low-speed wind tunnel using laser velocimetry. NASA TM 81165.

Stevenson, W. H., Thompson, H. D., and Roesler, T. C. (1982), Direct measurement of laser velocimeter bias errors in a turbulent flow. AIAA J. 20, pp. 1720-1723.

van de Hulst, H. C. (1957), Light Scattering by Small Particles. John Wiley and Sons, New York.

Yanta, W. J. and Lee, R. E. (1974), Determination of turbulence transport properties with the laser Doppler velocimeter and conventional time-averaged mean flow measurements at Mach 3. AIAA P-74-575.

Table 1. Particle response based on Stokes's drag law for $M_\infty = 3$, $T_E = 293°$ K and particles with a specific gravity of 1.

d_p (μm)	f_{3dB} (kHz)	x_c (mm)
5.0	0.9	110
2.0	5.4	18
1.0	22	4.4
0.5	86	1.1
0.3	239	0.4

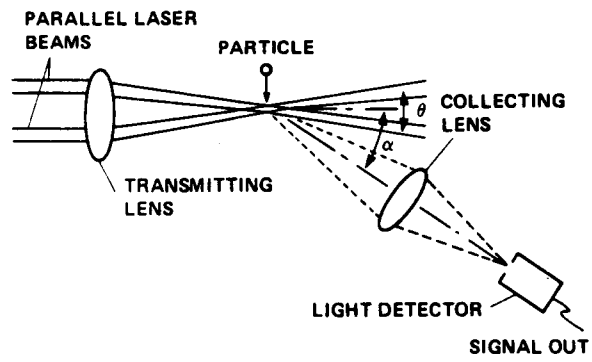

Figure 1. Simplified "dual-beam" laser Doppler anemometer.

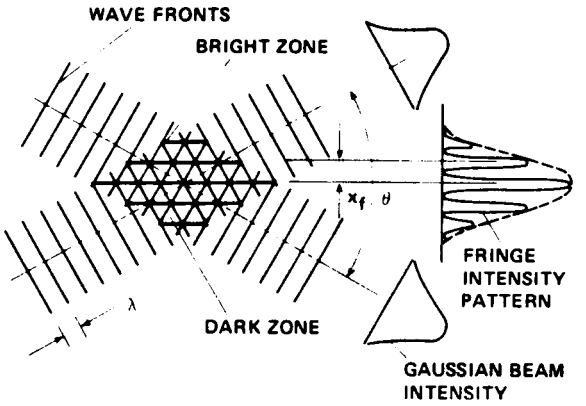

Figure 2. Depiction of fringe formation at beam crossover.

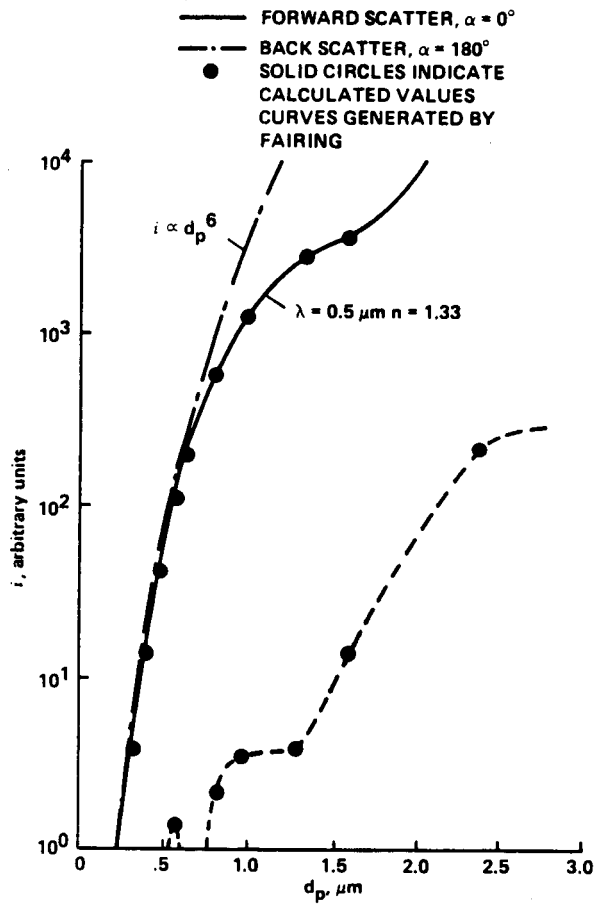

Figure 3. Calculated light scattering intensities for water droplets (n = 1.33) and 0.5 μm laser light. Calculated intensities taken from van de Hulst (1957) and Gumprecht et al. (1952).

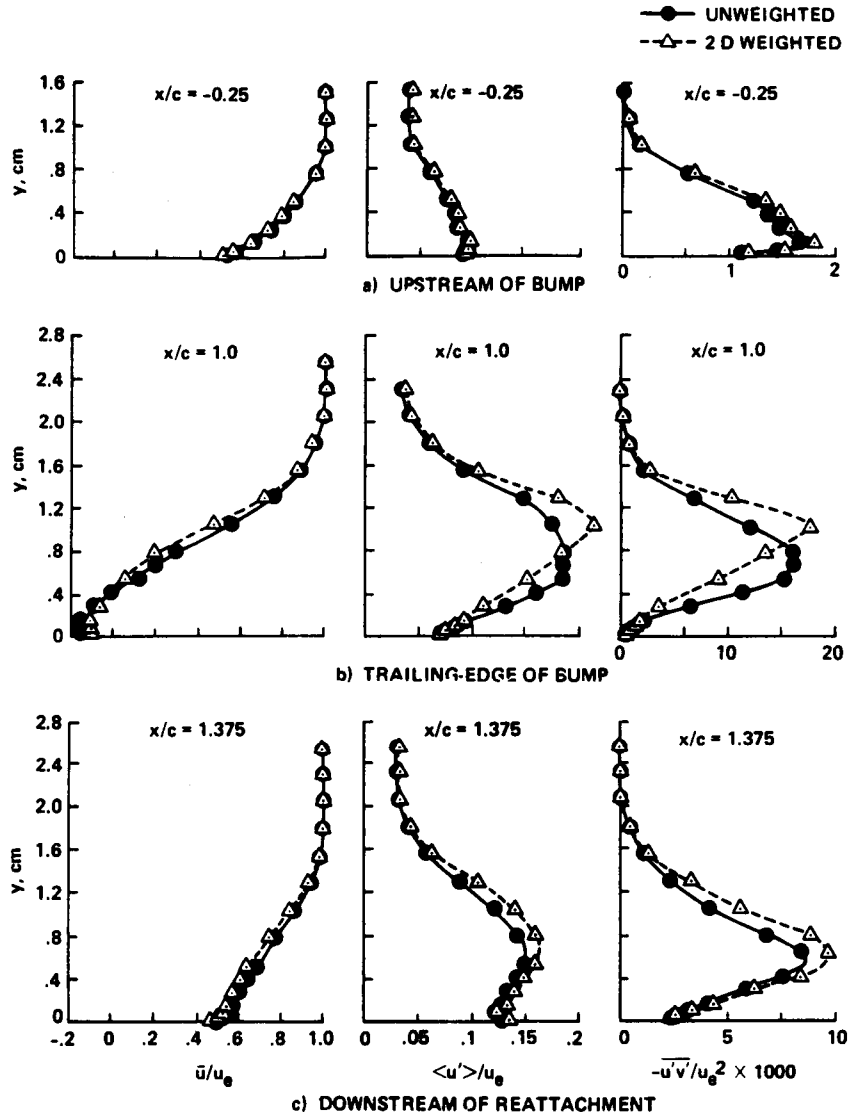

Figure 4. Uncorrected and bias-corrected results; axisymmetric bump model (M_∞ = 0.875).

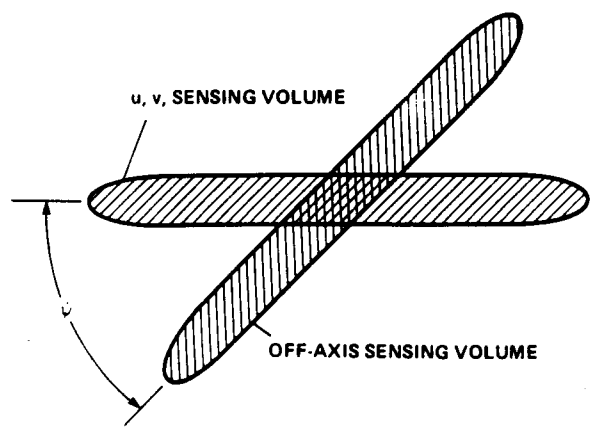

Figure 5. Overlapping sensing volumes for three-dimensional velocity measurements.

NASA
National Aeronautics and Space Administration

Report Documentation Page

1. Report No.	2. Government Accession No.	3. Recipient's Catalog No.
NASA TM-100072		

4. Title and Subtitle	5. Report Date
Laser Doppler Anemometry	June 1988
	6. Performing Organization Code

7. Author(s)	8. Performing Organization Report No.
Dennis A. Johnson	A-88101
	10. Work Unit No. 505-60-11

9. Performing Organization Name and Address	11. Contract or Grant No.
Ames Research Center Moffett Field, CA 94035	
	13. Type of Report and Period Covered
12. Sponsoring Agency Name and Address	Technical Memorandum
National Aeronautics and Space Administration Washington, DC 20546-0001	14. Sponsoring Agency Code

15. Supplementary Notes

Point of Contact: Dennis A. Johnson, Ames Research Center, MS 229-1
Moffett Field, CA 94035 (415) 694-5399 or FTS 464-5399

16. Abstract

The material in this NASA TM is to appear as a chapter on Laser Doppler Anemometry (LDA) in an AGARDograph entitled "A Survey of Measurements and Measuring Techniques in Rapidly Distorted Compressible Turbulent Boundary Layers" (H. H. Fernholz, A. J. Smits, and J. P. Dussauge, editors). The application of LDA (specifically, the dual-beam, burst-counter approach) to compressible flows is discussed. Subjects treated include signal processing, particle light scattering and tracking, data reduction and sampling bias, and three-dimensional measurements.

17. Key Words (Suggested by Author(s))	18. Distribution Statement
Laser Doppler anemometry Compressible flows Turbulence	Unclassified-Unlimited Subject Category - 34

19. Security Classif. (of this report)	20. Security Classif. (of this page)	21. No. of pages	22. Price
Unclassified	Unclassified	11	A02